

Label-free quantitative proteomic analysis reveals potential biomarkers and pathways in renal cell carcinoma

Zuohui Zhao · Fei Wu · Sentai Ding · Liang Sun ·
Zhao Liu · Kejia Ding · Jiaju Lu

Received: 12 August 2014 / Accepted: 30 September 2014 / Published online: 15 October 2014
© International Society of Oncology and BioMarkers (ISOBM) 2014

Abstract Renal cell carcinoma (RCC) is one of the most common malignancies in adults, and there is still no acknowledged biomarker for its diagnosis, prognosis, recurrence monitoring, and treatment stratification. Besides, little is known about the post-translational modification (PTM) of proteins in RCC. Here, we performed quantitative proteomic analysis on 12 matched pairs of clear cell RCC (ccRCC) and adjacent kidney tissues using liquid chromatography-tandem mass spectrometry (nanoLCMS/MS) and Progenesis LC-MS software (label-free) to identify and quantify the dysregulated proteins. A total of 1872 and 1927 proteins were identified in ccRCC and adjacent kidney tissues, respectively. Among these proteins, 1037 proteins were quantified by Progenesis LC-MS, and 213 proteins were identified as dysregulated proteins between ccRCC and adjacent tissues. Pathway analysis using IPA, STRING, and David tools was performed, which demonstrated the enrichment of cancer-related signaling pathways and biological processes such as mitochondrial dysfunction, metabolic pathway, cell death, and acetylation. Dysregulation of two mitochondrial proteins, acetyl-CoA acetyltransferase 1 (ACAT1) and manganese superoxide dismutase (MnSOD) were selected and confirmed by Western blotting and immunohistochemistry assays using another 6 pairs of ccRCC and adjacent tissues. Further mass spectrometry

analysis indicated that both ACAT1 and MnSOD had characterized acetylation at lysine residues, which is the first time to identify acetylation of ACAT1 and MnSOD in ccRCC. Collectively, these data revealed a number of dysregulated proteins and signaling pathways by label-free quantitative proteomic approach in RCC, which shed light on potential diagnostic or prognostic biomarkers and therapeutic molecular targets for clinical intervention of RCC.

Keywords Renal cell carcinoma · Acetylation · Label-free quantitative proteomics · Progenesis LC-MS

Introduction

Renal cell carcinoma (RCC) is the most common kidney cancer in adults, which is a very aggressive and sometimes fatal disease accounting for 3 % of all cancers [1–3]. In 2014, an estimated about 64,000 new cases and 14,000 RCC-specific deaths are expected in the US [3]. RCC is usually asymptomatic, but once some symptoms such as hematuria and flank pain occur, it indicates advanced or metastatic disease [1, 4]. Clear cell RCC (ccRCC) is the most common subtype, which accounts for 70–80 % of all renal masses. Clinically, nephrectomy remains the best option for localized RCC, which is associated with favorable prognosis (5-year survival rate ~85 %). Because RCC is resistant to chemotherapy and radiotherapy, prognosis is generally poor (5-year survival rate ~10 %) for patients with metastatic RCC (mRCC) or recurrent RCC, which are totally responsible for over 50 % of patients [1, 5]. Biological and targeted therapies have shown promising results [6, 7]; however, it is still a clinical challenge for these advanced RCC [1]. Systemic treatment for mRCC patients has shifted from cytokines to drug targeted therapies, which could improve progression-free survival, tumor response rate, or overall survival and health-

Electronic supplementary material The online version of this article (doi:10.1007/s13277-014-2694-2) contains supplementary material, which is available to authorized users.

Z. Zhao · S. Ding · L. Sun · Z. Liu · K. Ding · J. Lu (✉)
Department of Urology, Shandong Provincial Hospital Affiliated to
Shandong University, Jingwu Road, No. 324, Jinan,
Shandong 250021, China
e-mail: kyoto2310@sina.com

F. Wu
Department of Urology, Huashan Hospital, Fudan University,
Shanghai 200041, China

related quality of life [8]. Lack of biochemical markers to stratify patients into those who may or may not benefit from the systemic treatment is another challenge. Targeted therapy for advanced or metastatic RCC has benefited greatly from the discovery of two main abnormal signal transduction pathways—the mTOR signaling pathway and hypoxia-inducible pathway [4]. Owing to drug resistance and inevitable side effects, further study is required to find more targeted molecular biomarkers and signaling pathways to improve the overall prognosis for advanced RCC patients [4, 5]. It is still urgent to discover biomarkers and targets for early diagnosis, prognosis evaluation, monitoring for recurrence, and treatment stratification of patients with RCC [2].

Mass spectrometry (MS)-based proteomics has become an indispensable tool for biology, and it has been widely used in the study of protein-protein interactions, the mapping of numerous organelles, the description of specific species proteome, and the generation of quantitative protein profiles [9]. There are two basic workflows to interface with mass spectrometer for proteolysis: in-solution and in-gel digestion. The former can identify some hydrophobic, very high, or low molecular weight proteins and quantify most of the high-abundance proteins simultaneously. The latter can acquire higher sequence coverage and identify more post-translational modifications (PTMs) for the interested proteins [10]. PTMs of proteins perform significant influence on the cellular activity, stability, localization, and turnover [6]. Phosphorylation, glycosylation, acetylation, and nitration have been reported in association with the pathogenesis of cancers [11, 12]. Because protein acetylation at the epsilon amino group of lysine (Lys, K) neutralizes the positive charge, the reversible PTM usually regulates protein (especially histone) stability and protein-protein interactions [6]. Recently, increasing evidences have showed non-histone acetylation was associated with changing protein functions [13, 14], especially during metabolic regulation and autophagy controlling processes [15–17]. Interestingly, most proteins (especially enzymes) are acetylated which would presumably affect their structures and/or functions [14–16].

Proteomics is a promising alternative strategy to identify, quantify, and characterize a global set of proteins, especially discover the potential biomarkers or pathways for cancer in complex biological samples [6, 10]. And it has been used to identify differentially expressed proteins between RCC and normal kidney tissues, such as 60kD heat shock protein (HSPD1), ATP synthase subunit beta (ATP5B), and malate dehydrogenase (MDH), which might be potential candidates as diagnostic, prognostic markers, and therapeutic targets [2, 6, 18], but few reports about PTM of specific protein in RCC were elucidated [13, 19]. Recent studies have also reported some pathways such as mitochondrial dysfunction [4], glycolysis [18], metabolism [20], and protein transport [21] in RCC tissue or cell lines, whereas none of them is concerned

with PTM. Since lysine acetylation is a prevalent modification in organism, we speculate there are also some acetylated proteins in the pathogenesis and development of RCC.

In our previous study, we found that S(MeO)TLC, a novel Eg5-targeted drug, displayed potent anti-cancer efficacy in RCC *in vitro* and *in vivo* [7]. In order to find more therapeutic molecular targets and diagnostic or prognostic biomarkers, we performed label-free quantitative proteomic analysis to compare protein expression profiling and elucidate signaling pathways or biological processes between ccRCC and adjacent tissues, then selected a downregulated protein, acetyl-CoA acetyltransferase 1 (ACAT1), and an upregulated protein, manganese superoxide dismutase (MnSOD), to confirm their expression and regulation. These results might pinpoint some potential diagnostic or prognostic biomarkers and novel therapeutic targets for RCC.

Materials and methods

Clinical tissue samples

Eighteen cases of ccRCC and their morphologically normal kidney cortex adjacent to ccRCC (adjacent tissues) were collected from kidney cancer patients who underwent nephrectomy at the Department of Urology, Shandong Provincial Hospital Affiliated to Shandong University from December 2011 to January 2013. The 18 patients included 13 men and 5 women, with a mean age of 59 years (range 46–75 years). And they were graded according to the Fuhrman nuclear grade (G1: 4 cases, G2: 9 cases, G3: 4 cases, G4: 1 case) and staged according to the TNM classification (T1: 10 cases, T2: 6 cases, T3: 2 cases) [22]. Radiotherapy, chemotherapy, and immunotherapy were not performed before surgery, and all samples were verified by two pathologists after surgery. Kidney tissue samples were obtained with informed patient consent and approval of the hospital research ethics committee. The matched ccRCC and adjacent tissues were excised immediately following nephrectomy, cut into small blocks (~100 mg), rinsed with ice-cold PBS, snap-frozen in liquid nitrogen, and stored at -80°C until protein extraction and analysis.

Protein preparation

About 100 mg ccRCC or adjacent tissues were dissected, placed on ice, and homogenized in RIPA lysis buffer (Millipore, USA) containing protease inhibitor cocktail (Roche, Switzerland). The tissue lysates were centrifuged at 15,000g for 15 min at 4°C , and the supernatants were collected and stored in aliquots at -80°C . After protein concentration was determined using BCA protein assay (Bio-Rad, USA), the reference sample was prepared from a pool of 12

cases ccRCC or adjacent tissue lysates to avoid heterogeneity [10]. The other 6 cases kidney lysates were stored at -80°C for further confirmation: all 6 samples were used for immunoblotting and immunohistochemistry (IHC) assays; 4 samples were subjected to in-gel digestion of protein for MS analysis.

In-solution tryptic digestion

The pair of pool samples were processed in-solution digestion as previously described [21]. In brief, the samples were dialyzed with ammonium bicarbonate, reduced with DL-Dithiothreitol (DTT, Bio-Rad, USA), and alkylated with iodoacetamide (IAA; Sigma-Aldrich, USA). Trypsin (Sigma-Aldrich, USA) digestion was performed overnight, and Amicon C_{18} spin columns (Millipore, USA) were used to purify the peptides. Peptides were then dried in SpeedVac and stored at -80°C until analysis.

SDS-PAGE and in-gel tryptic digestion

About 100 μg protein from individual four patients lysates were run on 12 % sodium dodecyl sulfate polyacrylamide gel electrophoresis (SDS-PAGE). After Coomassie blue staining, the ACAT1 and MnSOD protein bands were cut from the gel, processed in-gel digestion with trypsin using the standard protocol [23]. After trypsin digestion, Ziptip C_{18} micropipette tips (Millipore, USA) were used to purify the peptides prior to adding 0.1 % formic acid for nanoLC-MS/MS analysis.

NanoLC-MS/MS analysis

Two independent protein tryptic methods (in-solution and in-gel digestion) were employed for liquid chromatography-tandem mass spectrometry (nanoLC-MS/MS) analysis. Peptides were fractionated by high pressure liquid chromatography (HPLC, Thermo EASY-nLC System, USA) interfaced with LTQ Velos Pro tandem mass spectrometer (Thermo Fisher Scientific, USA). The following LC buffers were used: buffer A (0.1 % (v/v) formic acid in Milli-Q water) and buffer B (0.1 % formic acid in 100 % acetonitrile). The peptides were eluted from the column at a constant flow rate of 300 nl min^{-1} with a linear gradient of buffer B from 5 to 35 % over 120 min. The MS parameters were set as follows: full scan by Velos followed by 20 LTQ MS/MS dependent scans with collision-induced dissociation (CID) mode. Every sample was run in quadruplicates with the same methods. The MS/MS data were analyzed with Proteome Discoverer 1.4 (Mascot and SEQUEST) according to the manufacturer's instruction and searched against the human protein database (UniProtKB, 2013.08.26, 72,275 sequences) for protein identification. Oxidation of methionine and acetylation of lysine were set as dynamic modification; carbamidomethylation of cysteine was

static modification. The threshold for accepting MS/MS spectra was false discovery rate (FDR) 0.05. For peptides modification identification, human UniProtKB MnSOD (P04179.2, SODM_human), ACAT1 (P24752, THIL_human) databases and Proteome Discoverer 1.4 (Sequest HT) were used. After four independent replicates running, all modification site assignments were confirmed by manual spectrum interpretation.

Label-free quantification

First, eight cases of in-solution digestion samples (ccRCC and adjacent tissue, $\times 4$ technical replicates) were acquired and analyzed in nanoLC-MS/MS. The acquired spectra (Thermo raw files) were loaded into the Progenesis LC-MS software (version 4.1; Nonlinear Dynamics, UK) and the ion intensity maps of all eight runs were examined for defects. Finally, six samples were chosen and label-free quantification was performed as previously described [4, 24]. One sample was set as the reference, data processing was aligned, and peptide ions (features) with charge state of +1 or >4 were excluded. Samples were then allocated to their experimental groups (ccRCC vs adjacent tissue). For quantification, the unique peptides validated by MS ($P < 0.05$) were chosen and calculated by summing the abundances of all peptides allocated to a specific protein [24].

Meanwhile, preliminary experiment discovered that MnSOD acetylation at lysine 68 (FDR < 0.05) was found in ccRCC instead of adjacent tissues. In order to compare the acetylation of MnSOD between ccRCC and adjacent tissues, in-gel digestion of MnSOD for MS analysis was also performed in quadruplicates and processed for Progenesis LC-MS analysis.

Pathway and network analyses of dysregulated proteins in ccRCC samples

Only the proteins that were quantified as unique non-redundant ones were retained in the subsequent analysis. Proteins were considered to be differentially expressed proteins if the difference was statistically significant ($P < 0.05$) by Progenesis LC-MS and the fold change > 1.5 or < 0.67 . The dysregulated proteins were chosen based on the criteria that the protein must be quantified by a minimum of three peptides, with > 95 % confidence and > 100 score, and ratio were > 1.5 or < 0.67 in ccRCC comparing with adjacent tissues (uncharacterized proteins and cDNA were also excluded). The dysregulated proteins were subjected to three pathway analysis tools: Ingenuity Pathway Analysis (IPA; Ingenuity Systems, USA), Search Tool for the Retrieval of Interacting Gene (STRING, version 9.0) and DAVID, for identifying enriched signaling pathways or networks and diseases categories [4].

IPA is a useful tool to model, analyze, and understand the complex biological system, especially reveal differentially regulated signaling networks and biological processes [18]. IPA core analysis workflow was performed on the differentially expressed or dysregulated proteins with default settings. Protein-protein interactions were visualized using the STRING database (<http://string-db.org/>) [25]. Parameters for species and confidence were “homo sapiens” and “medium confidence (0.400)”, respectively. STRING analysis was based on “confidence” mode, and disconnected nodes were hidden. The DAVID functional annotation tool (<http://david.abcc.ncifcrf.gov/>) uses over 40 annotation categories incorporating gene ontology, protein functional domains, and pathway databases to find enriched categories.

Western blotting analysis

Western blotting (WB) analysis was performed as previously described [23]. Kidney tissue lysates (50 µg each) were separated on SDS-PAGE, and the proteins in the gels were transferred to polyvinylidene difluoride (PVDF; Bio-Rad, USA) membranes. The membranes were detected with desired antibodies: anti-ACAT1 (dilution 1:1000, rabbit; Epitomics, USA), anti-MnSOD (dilution 1:750, mouse; Santa Cruz, USA), anti-acetyl lysine (dilution 1:1000, rabbit; Cell Signaling, USA), and anti-Tubulin (dilution 1:10,000, mouse; Sigma-Aldrich, USA), then fluorescence conjugated secondary antibodies (Li-Cor Biosciences, USA) were used to visualize the detected proteins. The blots were scanned with Odyssey infrared imaging system (Li-Cor Biosciences, USA).

Immunohistochemistry analysis

Kidney tissue hematoxylin-eosin (H&E) stained sections were reviewed by a pathologist to identify representative areas of the tumors. Immunohistochemistry (IHC) analysis was performed as previously described [26]. The slides were stained with anti-MnSOD (dilution 1:50) and anti-ACAT1 (dilution 1:50) antibodies using an Envision⁺-based detection system and developed with diaminobenzidine (DAB; Zhongshan, China). Negative controls were performed by omitting the primary antibody.

Data analysis

SPSS 17.0 software (SPSS Inc., USA) was used for statistical analysis. $P < 0.05$ was considered statistically significant. Statistical analyses between two groups were performed using a two-tailed Student's *t* test, whereas comparisons involving multiple groups were performed with a two-way ANOVA test.

Results

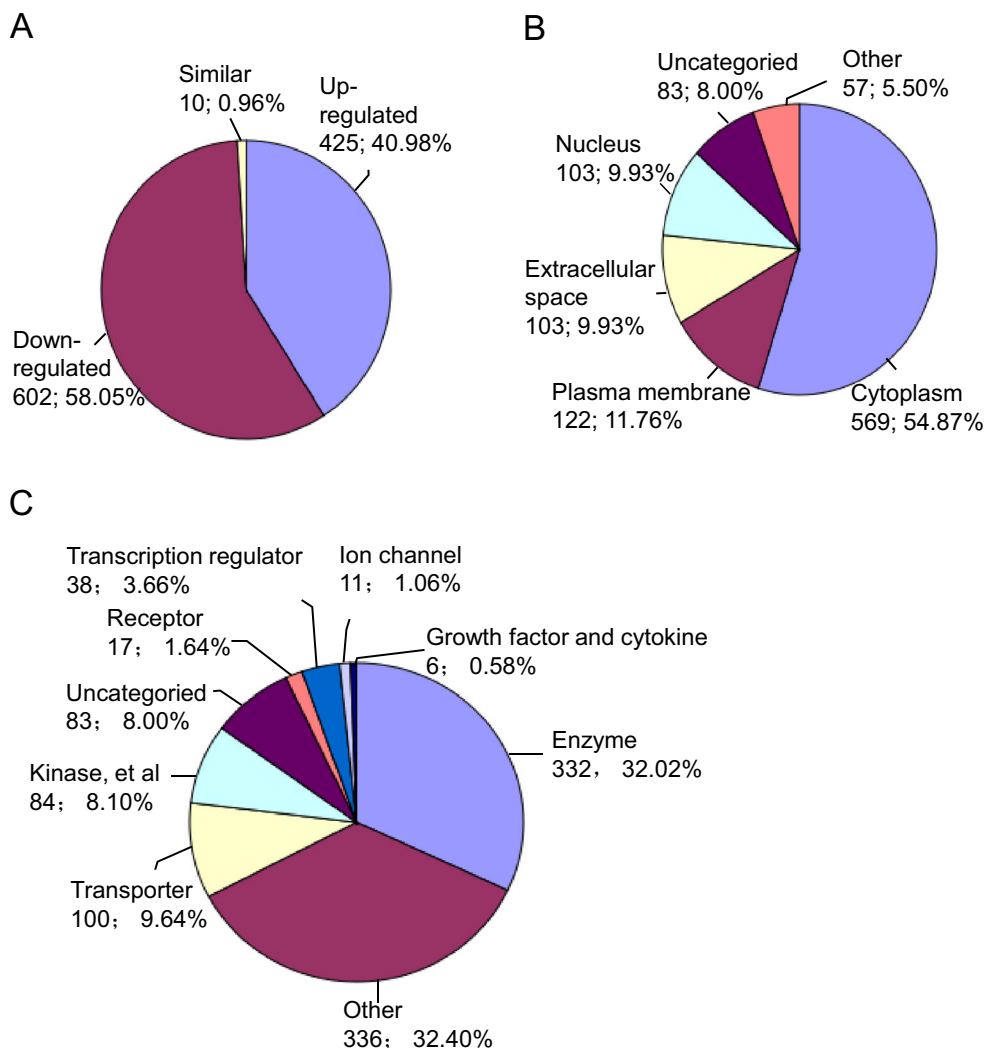
Identification and quantification proteins between ccRCC and adjacent tissues

Twelve pairs of kidney tissues were used and a pair of pool samples was constructed according to their protein concentrations. After in-solution tryptic digestion, the samples were analyzed in quadruplicates by nanoLC-MS/MS. A total of 1872 and 1927 proteins were identified in ccRCC and adjacent tissues, respectively (Online Resource 1). After evaluating the MS data quality of all eight samples, six samples were chosen and performed for label-free quantitative analysis with Progenesis LC-MS software, using an algorithm based on the pairwise features detection at the LC-MS level [24]. The label-free analysis showed 1037 proteins were reliably quantified in all the three biological replicates ($P < 0.05$, Online Resource 1). Of the 1037 proteins, 425 proteins were upregulated (40.98 %, ratio > 1.5), 10 proteins were unchanged (0.96 %), and 602 proteins were downregulated (58.05 %, ratio < 0.67) in ccRCC (Fig. 1a). IPA protein classification (Fig. 1b, Online Resource 2) showed that the main protein locations were the cytoplasm (569, 54.87 %) and plasma membrane (122, 11.76 %), then the extracellular space (103, 9.93 %) and nucleus (103, 9.93 %). As shown in Fig. 1c, the cellular molecular function analysis revealed that there were 332 regular enzymes (32.02 %) and 84 kinase/peptidase/phosphatases (8.10 %), 100 transporters (9.64 %), and 38 transcription regulators (3.66 %).

Pathway, process, and protein-protein interaction analyses of dysregulated proteins between ccRCC and adjacent tissues

In total, we identified 1027 differentially expressed proteins ($P < 0.05$). Among these proteins, 213 proteins met the criteria for dysregulation between ccRCC and adjacent tissues: 64 were upregulated (ratio > 1.5) and 159 were downregulated (ratio < 0.67) in ccRCC (Online Resource 1). First, we elucidated the role of these proteins in ccRCC pathogenesis and identified pathways of carcinogenesis that can be candidates as the diagnostic markers and/or therapeutic targets. The dysregulated proteins were subjected to IPA analysis, which was used to investigate the functional aspects of the dysregulated proteins. Figure 2a showed the heatmap of “diseases and function” pathway which the 213 dysregulated proteins were involved in, developmental and hereditary disorder, cell death and survival, neurological disease, metabolic disease, and psychological disorder ranked the top five diseases or functions (Online Resource 2). As shown in Fig. 2b, mitochondrial dysfunction [4, 18] (24 proteins), oxidative phosphorylation (16 proteins), and fatty acid β -oxidation I (9 proteins) ranked the top three canonical pathways, after that were macromolecules degradation and glycolysis or glycogenesis, which is

Fig. 1 Mass spectrometry-based quantitative proteomic analysis of human kidney proteins. Proteins were isolated from ccRCC and adjacent tissues, and they were subjected to nanoLC-MS/MS for protein identification. After Progenesis LC-MS analysis, 1037 proteins were quantified and processed to IPA classification. **a** Expression profiling of the 1037 proteins. **b** Subcellular distribution of the 1037 proteins. **c** Functional category of the 1037 proteins



consistent with previous reports [10]. In addition, most of the canonical pathways (96.0 %) connected to one main cluster among the top 25 pathways (Fig. 2c), which indicated that the dysregulated molecules formed a systematic dynamic network and an interconnected signaling network during the ccRCC pathogenesis.

IPA function analysis also displayed that 213 dysregulated proteins were involved in some tumorigenesis-related processes (Table 1, Online Resource 2). One hundred six proteins were found to regulate cell death process. For example, heat shock protein 90kD alpha (HSP90AA1) is required for the survival and proliferation of ovarian cancer cell SKOV3, and it also increases chemoresistance to cisplatin [27]. Ninety-seven proteins played a vital role in cellular proliferation process. For instance, catalase (CAT) promotes cell growth; transforming growth factor beta 1 (TGF β 1) has been identified as a promising prognosis marker of ccRCC recently [28]. One hundred thirty-four proteins were involved in the carcinogenesis. Recent study indicated ACAT1, a key enzyme of ketogenic pathway, was associated with prostate

cancer progression [26]. Thirty-two proteins and 18 proteins were involved in the fatty acid and amino acid metabolism, respectively, which both belonged to vital metabolic processes. The top four networks of the dysregulated proteins were metabolic disease, energy production, cell morphology, and free radical scavenging (Online Resource 2).

Protein-protein interaction for dysregulated proteins was also visualized using STRING analysis, and one main interactive cluster was formed among these proteins (Fig. 3), which indicated the protein-protein interaction network was enriched within this protein set. Some known important proteins or key enzymes, like CAT, MnSOD, myeloperoxidase (MPO), lactate dehydrogenase (LDH), TGF β 1, and ATP synthase F1 complex alpha subunit 1 (ATP5A1), were dispersed and located in the notes of the network. The KEGG pathway analysis using STRING also yielded similar networks (Online Resource 3), pinpointing the most significant pathways including metabolic pathway and oxidative phosphorylation. The DAVID functional annotation tool (Table 2, Online Resource 3) showed 118 proteins participated in

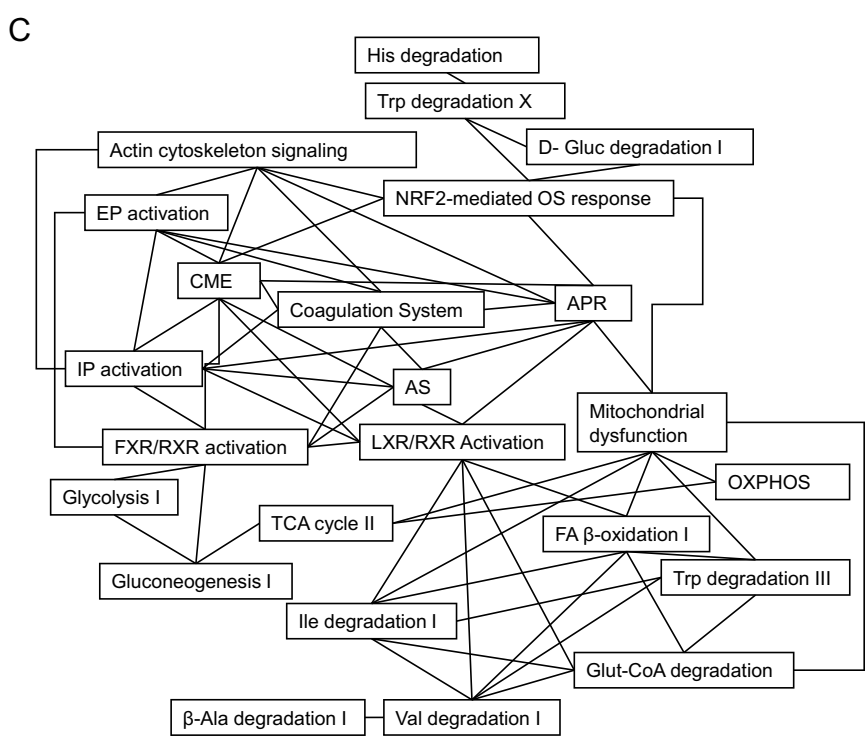
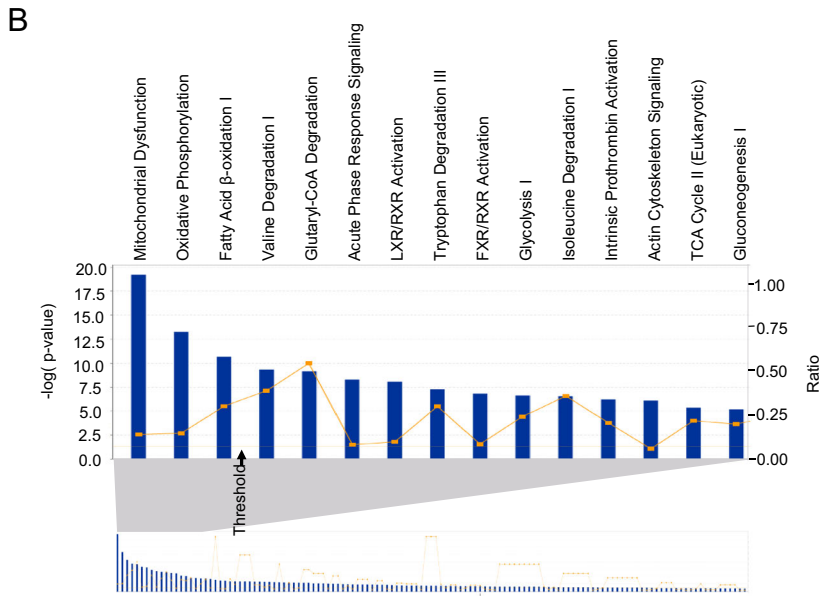
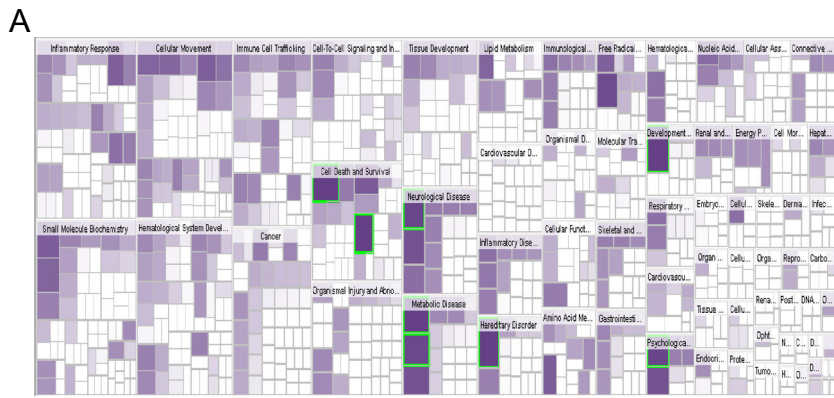


Fig. 2 IPA core analysis of the 213 dysregulated proteins between ccRCC and adjacent tissues. **a** IPA core analysis was performed on the dysregulated proteins and the heatmap showed the disease and function pathway. The color increased by *P* value and green box displayed the top pathways. **b** IPA core analysis revealed the top canonical pathways that were enriched in the 213 dysregulated proteins (only top 15 pathways displayed). **c** IPA canonical pathways interconnected and formed one main cluster (only top pathways displayed). The connections between nodes represented shared proteins. *APR* acute phase response signaling, *Ala* alanine, *AS* atherosclerosis signaling, *CME* clathrin-mediated endocytosis signaling, *EP* extrinsic prothrombin, *FA* fatty acid, *Gluc* glucuronate, *Glut* glutaryl, *His* histamine, *IP* intrinsic prothrombin, *Ile* isoleucine, *OXPHOS* oxidative phosphorylation, *OS* oxidative stress, *Trp* tryptophan, *Val* valine

acetylation modification ($P=3.57e^{-49}$), a pivotal PTM in regulating cell metabolism and autophagy [15–17]. ACAT1 has been reported to be acetylated at lysine 174 in the literature [16]. Sixty-five proteins were located in the mitochondrion ($P=6.58e^{-40}$), especially for some key enzymes, such as MnSOD and CAT, which play the vital role for mitochondrial reactive oxygen species (ROS) balance. And 75 proteins mutated during disease conditions ($P=1.49e^{-29}$), for example, ceruloplasmin is over-expressed in obesity-associated cancer [29].

Validation of dysregulated proteins between ccRCC and adjacent tissues

Among the 213 dysregulated proteins identified by the pooled 12 patients samples between ccRCC and adjacent tissues, two mitochondrial proteins, ACAT1 and MnSOD, were chose to validate their differential expressions by immunoblotting and IHC assays in another six individual samples. We chose ACAT1 as a candidate to be validated because it is a key enzyme which participates in the fatty acid metabolism (especially ketogenic pathway) and protein acetylation [26, 30], and it is a potential prognostic marker in prostate cancer [30]. We chose MnSOD as a candidate because it is a ubiquitous

antioxidant metalloenzyme and is essential for the development and progression of cancer [31]. In addition, both of them have been reported to be acetylated at lysine residues in the literature [16].

As shown in Fig. 4a, a significant downregulation of ACAT1 expression in ccRCC was detected in all six samples (0.41 fold, $P<0.05$), compared with adjacent tissues. Meanwhile, there was a significant upregulation of MnSOD expression in ccRCC (1.71 fold, $P<0.05$). The IHC also showed that strong positive cytoplasmic staining for ACAT1 was confined in kidney tubule epithelium cells and only weak positive or negative staining in ccRCC cells; MnSOD strong positive cytoplasmic staining was seen in the majority of the ccRCC cells and part of normal kidney tubule epithelium cells, but not in normal glomerular epithelial cells (Fig. 4b), which also verified both the MS and immunoblotting results.

The MS/MS spectra showed the involvement of two acetylated lysine residues, Lys-174 (ACAT1) and Lys-130 (MnSOD), present in both ccRCC and adjacent tissues, while high confidence Lys-68 (MnSOD) was only found in ccRCC (Fig. 5a–c). WB also displayed that there was evident acetylation signal corresponding to MnSOD protein band in ccRCC (Fig. 5d). In order to compare acetylation difference of MnSOD between ccRCC and adjacent tissues, MnSOD was processed to Progenesis LC-MS analysis after in-gel tryptic digestion and nanoLC-MS/MS. The peptide quantification for MnSOD showed both the acetylated peptides (containing Lys-68 and Lys-130) increased in proportion with MnSOD protein (Fig. 5e), which indicated that the acetylated MnSOD might play an important role in both ccRCC and normal kidney.

Collectively, these data not only confirmed our proteomics results, but also indicated that ACAT1 and MnSOD expression or their acetylation might play an important role in the ccRCC pathogenesis. Whether ACAT1 and MnSOD might be prognostic markers for ccRCC using IHC is in progress.

Table 1 IPA molecular and cellular function analysis of dysregulated proteins^a

Tumorigenesis-related processes	Protein #	<i>P</i> value	Protein symbol ^b
Cell death	106	5.91E-18	ACAT1, ACLY, ACTC1, ACTN4, AIFM1, ALB, ALDH2, ANPEP, ANXA1, ANXA2, ANXA4, APOA1, APOB, APOE, HSP90AA1...
Cellular proliferation	97	2.72E-11	ACAT1, ACLY, ACTG1, ACTN4, AHNAK, AK2, AK4, ALB, ANPEP, ANXA1, ANXA2, APOA1, APOE, TGF β1, CAT...
Carcinoma	134	1.39E-07	ABAT, ACAA2, ACADVL, ACAT1, ACLY, ACSM2B, ACTC1, ACTG1, ACTN4, ACY1, AHNAK, AIFM1, AK4, ALB, ANXA3...
Amino acids metabolism	18	5.62E-13	ABAT, ALDH6A1, ASS1, BHMT, DDC, DMGDH, FTCD, GATM, GGT1, GLS, GLUD1, GLYAT, GOT2, HIBADH, MCCC2...
Fatty acid metabolism	32	3.21E-12	ABAT, ACAA1, ACAA2, ACADVL, ACLY, ALB, ANXA1, APOA1, APOB, APOE, ATP5J, C5, COTL1, EC12, EHHADH...

^a 213 dysregulated proteins between ccRCC and adjacent tissues were input into Ingenuity Pathway Analysis (IPA), core analysis result

^b Protein symbols were used according to UniProtKB/Swiss-Prot and only 15 proteins are displayed in the table. For full protein names and other details, see Online Resource 2

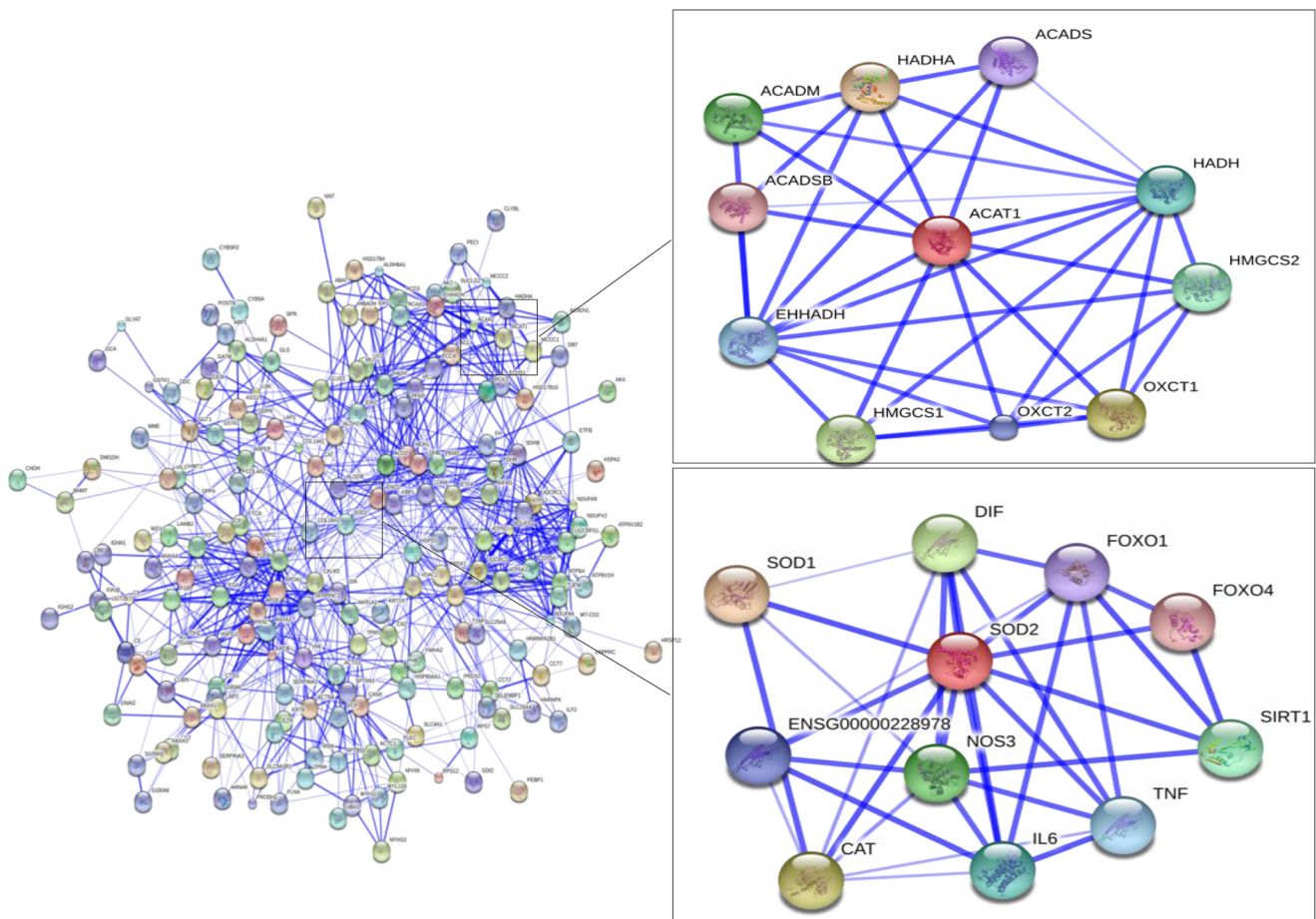


Fig. 3 Visualization of protein-protein interactions of the dysregulated proteins in ccRCC using STRING analysis (confidence mode). Two hundred thirteen proteins were input into STRING software and they formed one main cluster. Lines represented interactions between proteins

and thickness denoted the confidence level associated with each interactions. Two mini-clusters displayed the two candidate proteins (red spheres in the middle of clusters), which were located in the network and were chosen to be validated later

Discussion

High-throughput proteomics has the remarkable ability to capture changes in thousands of variables simultaneously

between normal and diseased conditions [4]. Recently, quantitative proteomic approaches, such as isotope-code affinity tag (ICAT) and more convenient label-free quantitative strategies, have been widely used to identify and quantify proteins

Table 2 David functional annotation analysis of dysregulated proteins^a

Category	Protein #	P value	Protein symbol ^b
Acetylation	118	3.57E-49	ACAT1, SPTBN1, GLUD1, HIST1H2BK, APOB, CHDH, HSD17B10, ALDH6A1, CYB5A, NDUFA4, SLC4A1, PFN1, ABAT, AK2, QDPR ...
Mitochondrion	67	6.58E-40	ACAT1, ACADVL, GLUD1, CHDH, HSD17B10, ALDH6A1, IDH2, NDUFA4, VDAC1, AIFM1, MCCC2, DMGDH, ABAT, AK2, SUCLG2...
Transit peptide	54	3.53E-39	ACAT1, ACADVL, GLUD1, CHDH, ALDH6A1, IDH2, AIFM1, MCCC2, DMGDH, ABAT, SUCLG2, PCK2, ATP5J, ETFA, GATM...
Disease mutation	75	1.49E-29	ACAT1, ACADVL, SLC9A3R1, GLUD1, APOB, HSD17B10, ALDH6A1, GSN, SLC4A1, MCCC2, DMGDH, CUBN, ABAT, AK2, QDPR...
Oxido-reductase	46	5.97E-27	ACADVL, HSD17B4, GLUD1, CHDH, HSD17B10, ALDH6A1, IDH2, CAT, ALDH2, MPO, AIFM1, DMGDH, AOC1, QDPR, CP...

^a 213 dysregulated proteins between ccRCC and adjacent tissues were input into DAVID, protein functional annotation chart

^b Protein symbols were used according to UniProtKB/Swiss-Prot and only 15 proteins displayed in the table. For full protein names and other details, see Online Resource 3

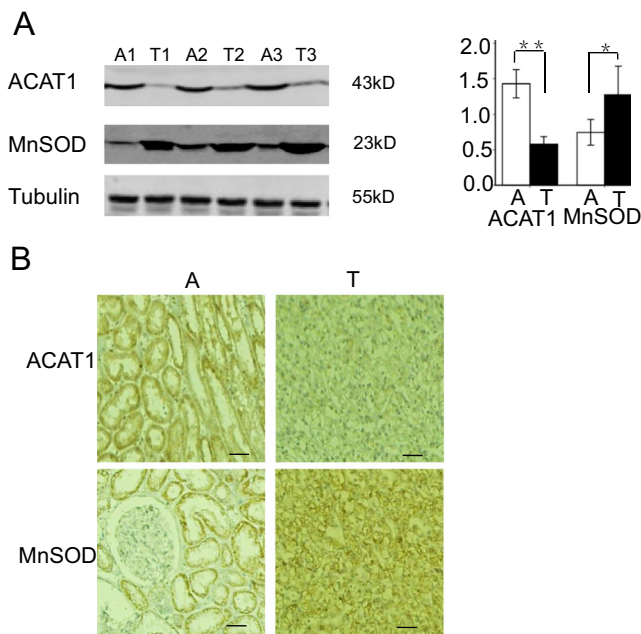


Fig. 4 Validation ACAT1 and MnSOD expression dysregulation in adjacent (A) and ccRCC (T) tissues by Western blotting (WB) and immunohistochemistry (IHC) assays. **a** Representative blots validated ACAT1 downregulation and MnSOD upregulation in ccRCC ($n=6$). Tubulin served as the loading control. * $P < 0.05$, ** $P < 0.01$. **b** Representative photomicrographs verified ACAT1 and MnSOD dysregulation in adjacent (A) and ccRCC (T) tissues (original magnification, 200 \times ; bars=50 μm)

in complex biological samples, and they also have been used to understand molecular mechanism of diverse diseases. Label-free quantitative proteomics has become a potent screening tool in biomarker and pathway discovery [4]. Even low-abundance peaks fail to obtain MS/MS information or only have poor MS/MS signals (like Lys-68 in adjacent tissues), Progenesis LC-MS still can retrieve their MS data from other highly expressed samples and quantify their abundance, because this software utilizes “match between runs” algorithm to maximize the quantification information. In the present study, we utilized label-free quantitative proteomic approach to profile the proteome of ccRCC and adjacent tissues. Specifically, we identified over 1800 proteins, quantified 1037 non-redundant proteins, and pinpointed 213 dysregulated proteins between ccRCC and adjacent tissues.

Several proteomic studies about kidney cancer have been reported recently, most of which identified some pathways such as glycolysis, metabolism, mitochondrial dysfunction and validated two or more dysregulated proteins expression [4, 18, 20, 21]. But none of them referred to PTMs (including acetylation) of proteins in RCC, and almost all of them focused on over-expressed proteins in RCC. Another feature in our study included simultaneous profiling of multiple admixed specimens, which could avoid heterogeneity and remove artifactual differences owing to differential protein losses during proteins or peptides preparation [10], though

more specimens from kidney patients were needed to confirm our results. Some of the dysregulated proteins discovered by other groups using quantitative proteomic approach are consistent with the findings reported here, such as thymidine phosphorylase (TP), periostin (POSTN), annexin A4 (ANXA4) [4], CAT, glyceraldehyde-3-phosphate dehydrogenase (GAPDH), 3-ketoacyl-CoA thiolase (HADHA), alpha-enolase (ENO1), L-lactate dehydrogenase A (LDHA), ACAT1 [10], ATP5A1, and HSP90AA1 [18], and some of them has been validated by immunoblotting or IHC assays. Many of them might become potential prognostic and therapeutic biomarkers for clinical intervention of RCC, for example, TGF β 1, a dysregulated protein found in our experiment set, has been identified as a promising prognosis marker of ccRCC recently [28].

Given the large number of dysregulated proteins in ccRCC and adjacent tissues, ACAT1 and MnSOD, which were both located in the nodes of network and had been reported to be related with human cancer, were selected, and their validation by Western blotting and IHC analyses would confirm their relevance in the biological network. Lysine acetylation is a prevalent modification in metabolic enzymes that affect their activities or stabilities [14–16, 32]; previous report noted both ACAT1 and MnSOD were acetylated at lysine residues in liver tissues [16], whether they were acetylated in ccRCC is still unknown.

ACAT1 is involved in the formation and degradation of ketone bodies, and defects in ACAT1 lead to 3-ketothiolase deficiency (3KTD), which is characterized by ketoacidotic attacks [33]. In prostate cancer, recent studies demonstrated that ACAT1 increased in androgen-independent LNCaP-SF comparing with LNCaP cell line, and it was associated with prostate cancer progression [26, 30]; further study showed ACAT1 could serve as a potential prognostic marker in prostate cancer [30]. In kidney cancer, White et al. found that ACAT1 was decreased in ccRCC comparing with adjacent tissues using quantitative proteomic approach [10], which is consistent with our result. The IPA canonical pathway showed that all the proteins involved in ketogenesis decreased simultaneously in ccRCC, either in the quantitative 1037 proteins (including BDH2, BDH1, ACAT1, HMGCL, HADHA) or in the dysregulated 213 proteins (including ACAT1, HADHA), and Western blotting and IHC also confirmed that ACAT1 down-expressed in ccRCC, which indicated that ketogenic pathway might be different between kidney cancer and prostate cancer. There are many lipid droplets within ccRCC cytoplasm [1], whether ACAT1 also participates in cholesterol metabolism, like cytosolic acetyl-Coenzyme A acetyltransferase 2 (ACAT2), is still unknown. Novel role of ACAT1 as an acetyltransferase has been identified in mammalian cells [34]. Since ACAT1 is downregulated in ccRCC, whether ACAT1 might be a favorable prognostic marker and over-expressing ACAT1 in cancer cells might

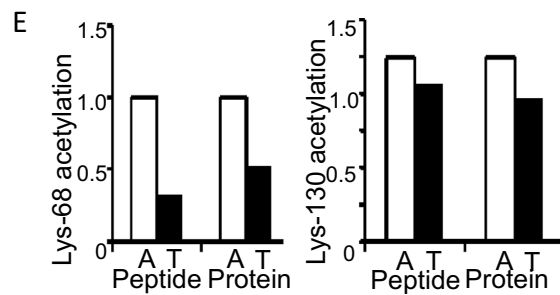
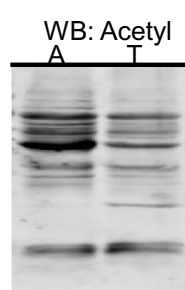
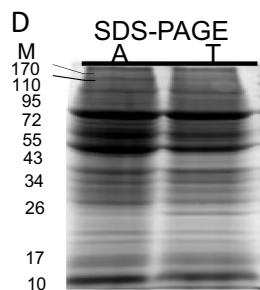
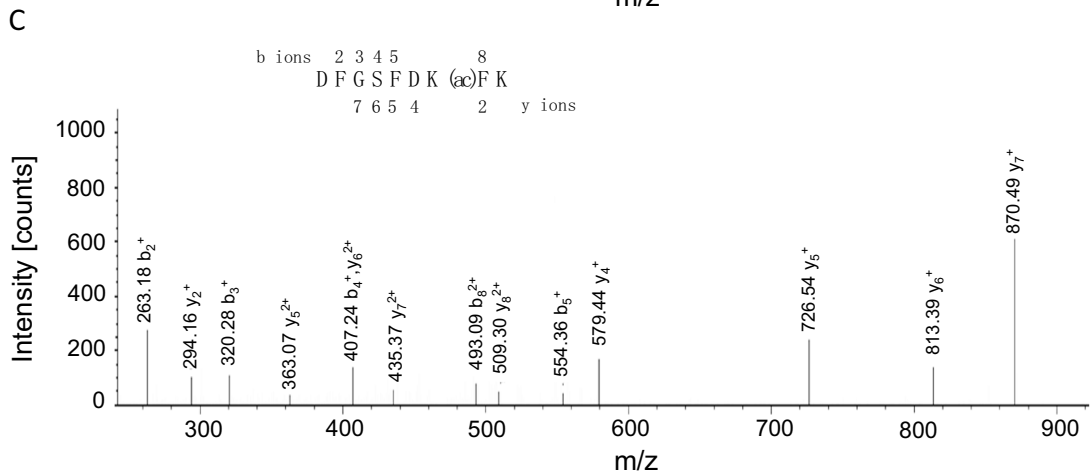
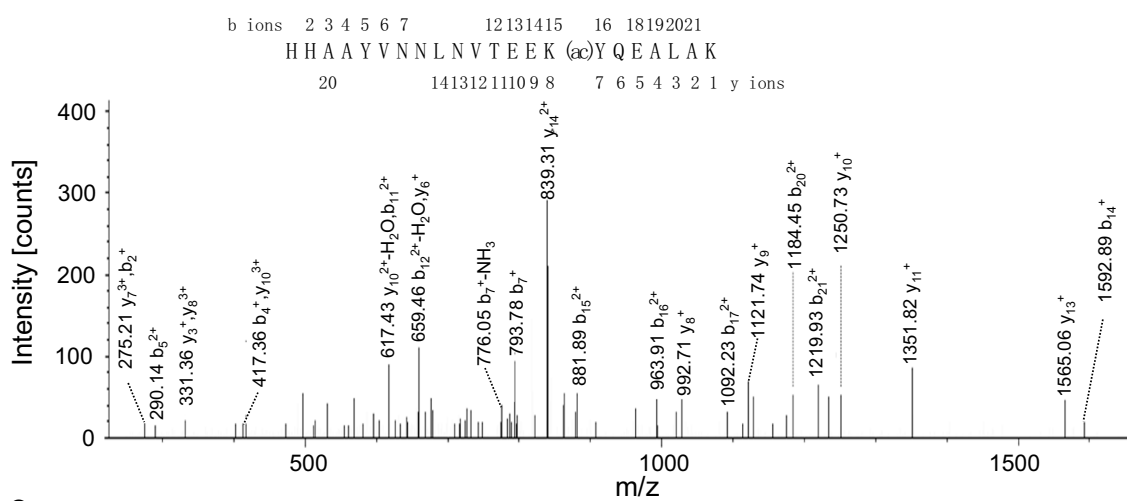
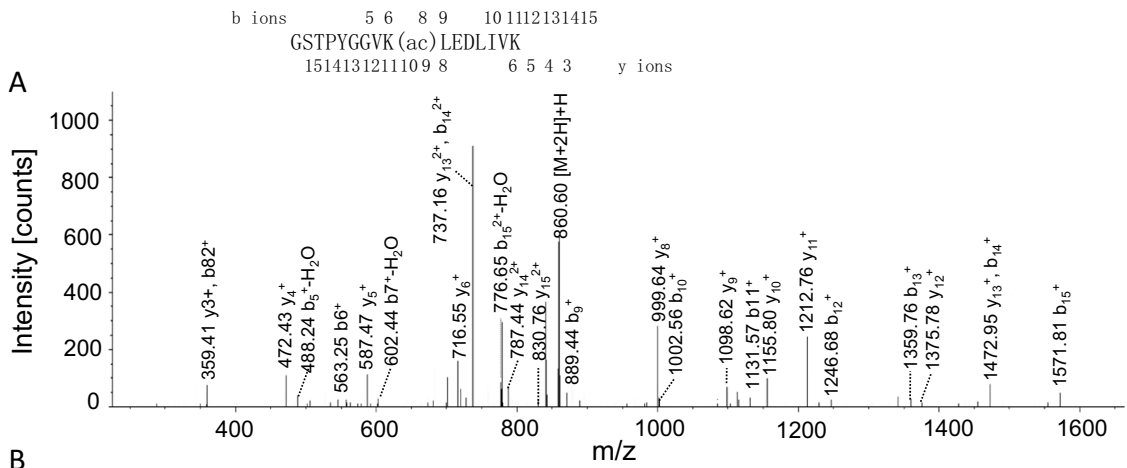


Fig. 5 Validation ACAT1 and MnSOD acetylation in ccRCC specimens by MS. **a** The mass spectrum showed ACAT1 acetylation at lysine 174. **b** The mass spectrum showed MnSOD acetylation at lysine 68. **c** The mass spectrum showed MnSOD acetylation at lysine 130. *m/z* mass-to-charge ratio. Only the detected y and b ions are labeled. **d** WB revealed protein acetylation profiling difference between adjacent (*A*) and ccRCC (*T*) tissues. The SDS-PAGE (*left*) and WB against anti-acetyl antibody (*right*) showed different acetylation profiling of the pool samples from adjacent and ccRCC tissues. *M* marker. *Arrow* indicated two candidate proteins. **e** Acetylated Lys-68 and Lys-130 of MnSOD in adjacent (*A*) and ccRCC (*T*) tissues were quantified using Progenesis LC-MS software. The average normalized abundances of acetylated Lys-68 and Lys-130 were calculated by the ratio of the relative signal between the peptide HHAAYVNNLNVTEEK68(ac)YQEALAK, DFGSFDK130(ac)FK and the total peptide HHAAYVNNLNVTEEKYQEALAK, DFGSFDKFK or total protein. According to Progenesis LC-MS, the average abundances of acetylated and total Lys-68 were 1.36e+4 and 4.37e+4, acetylated and total Lys-130 were 5.43e+3 and 2.44e+4, and total protein were 2.54e+6 and 1.47e+7, respectively. ($n=3$, ANOVA test)

restore growth characteristics of the normal cells still need to be further studied.

MnSOD is a potent scavenger of superoxide radicals and plays a central role in the defense against oxidative stress that is linked to aging and cancer [31]. The role of MnSOD in carcinogenesis has been widely studied [35, 36], and many studies found that increased MnSOD expression was associated with cancer metastasis and poor prognosis [37]. Previous studies focused on MnSOD tyrosine (34) nitration and its enzyme activity [38]. Recent studies also found that MnSOD acetylation at lysine residues also inactivated its enzyme activity, and Sirt3 deacetylated MnSOD in the mitochondria and increased its activity, but most of them were concerned with MnSOD knockout mouse embryonic fibroblasts (MEFs), Sirt3 knockout MEFs, or mice [14, 32, 39], no one reported MnSOD acetylation in ccRCC. We not only identified the two lysine acetylated sites (Lys-68 and Lys-130) of MnSOD in ccRCC, but also quantified and compared its acetylated peptides. MnSOD expression was higher in ccRCC than adjacent tissues (Fig. 4a), but the ratio of acetylated MnSOD was similar (Fig. 5e), which indicated that the acetylation might participate in regulating MnSOD activity in both ccRCC and normal kidney. Cancer cells produce more ROS than their corresponding normal cells, and more MnSOD aggregates in ccRCC to scavenge ROS. Targeting MnSOD and reversing its expression have been a promising approach to the selective killing of cancer cells or inhibiting tumor growth [40].

Pathway analysis provides us an approach to identify enrichment of various signaling pathways from the differentially expressed or dysregulated proteins, which might play the key roles in tumorigenesis or cancer progression. A number of pathways such as mitochondrial dysfunction [4, 18], glycolysis, and metabolic pathways [10, 20] reported previously were confirmed by our data. Mitochondrial dysfunction pathway, enriched in the IPA analysis, could be a novel potential therapeutic target in RCC. Many of the other pathways enriched in

IPA analysis, such as oxidative phosphorylation, cell death and survival, free radical scavenging, and amino acid metabolism, all are more or less concerned with mitochondrion. The mitochondria play important roles in cellular energy metabolism, free radical generation, and apoptosis [41], and they integrate many signaling pathways important for the life and death of cells [31]. Abnormal mitochondrial function is common in cancer cells, and it also activates pathways which are suppressed in normal cells. Growing evidences have shown that the mitochondria might serve as targets for anti-cancer therapies [42]. Lysine acetylation, the reversible PTM of protein, also plays a vital role in RCC cancerogenesis. To date, the majority of research on lysine acetylation has focused on histone and their relationships with RCC [19]. For example, MYST1, as an acetyltransferase of H4K16, might be a new RCC diagnostic maker [43]; histone H3 acetylation is responsible for preserving chronic mTOR inhibitor sensitivity in RCC [44]. However, there is a growing evidence that non-histone acetylation also participates in RCC pathogenesis. Noh et al. recently reported that acetylated P53 indicated favorable prognosis in ccRCC [13]. Reversing the epigenetic modifications of their target proteins has the potential to reactivate tumor suppressor genes or suppress oncogenes, thus, inhibit tumor growth or progression [19]. For example, the decreased acetylation of histone H3 is a common alteration in RCC, and increasing the amount of acetylated histone H3 might be a therapeutic option for RCC [45]. The acetylation of ACAT1 and MnSOD had not been reported in RCC before, and the two candidate proteins or their acetylated sites might become potential therapeutic targets for RCC. The 67 dysfunctional mitochondrial proteins and 118 acetylated proteins, together with other dysregulated proteins, which are involved in cancer-related pathways, might serve as potential therapeutic molecular targets for RCC.

Collectively, through label-free quantitative proteomic analysis, we identified a number of differentially expressed or dysregulated proteins, such as ACAT1 and MnSOD, which are involved in carcinogenesis and have the potential to become diagnostic, prognostic, and stratification treatment biomarkers in ccRCC. In addition, we disclosed many signaling pathways and biological processes which were activated in ccRCC, and these dysregulated pathways or processes, like mitochondrial dysfunction and acetylation, might become novel therapeutic targets for ccRCC, which might greatly improve patient prognosis and increase overall survival, especially for unresectable RCC.

Acknowledgments This study was supported in part by the grants from the National Natural Science Foundation of China (No. 81202017) and the Natural Science Foundation Shandong Province (No. ZR2011HQ027).

Conflicts of interest None.

Ethics statement All procedures were consistent with the National Institutes of Health Guide and approved by the institutional board with patients' written consent. This study was evaluated and approved by the Ethics Committee of Shandong Provincial Hospital Affiliated to Shandong University.

References

- Rini BI, Campbell SC, Escudier B. Renal cell carcinoma. *Lancet*. 2009;373(9669):1119–32. doi:10.1016/S0140-6736(09)60229-4.
- Craven RA, Stanley AJ, Hanrahan S, Dods J, Unwin R, Totty N, et al. Proteomic analysis of primary cell lines identifies protein changes present in renal cell carcinoma. *Proteomics*. 2006;6(9):2853–64. doi:10.1002/pmic.200500549.
- Siegel R, Ma J, Zou Z, Jemal A. Cancer statistics, 2014. *CA Cancer J Clin*. 2014;64(1):9–29. doi:10.3322/caac.21208.
- Atrih A, Mudaliar MA, Zakikhani P, Lamont DJ, Huang JT, Bray SE, et al. Quantitative proteomics in resected renal cancer tissue for biomarker discovery and profiling. *Br J Cancer*. 2014;110(6):1622–33. doi:10.1038/bjc.2014.24.
- Gupta K, Miller JD, Li JZ, Russell MW, Charbonneau C. Epidemiologic and socioeconomic burden of metastatic renal cell carcinoma (mRCC): a literature review. *Cancer Treat Rev*. 2008;34(3):193–205. doi:10.1016/j.ctrv.2007.12.001.
- Janech MG, Raymond JR, Arthur JM. Proteomics in renal research. *Am J Physiol Ren Physiol*. 2007;292(2):F501–12. doi:10.1152/ajprenal.00298.2006.
- Ding S, Zhao Z, Sun D, Wu F, Bi D, Lu J, et al. Eg5 inhibitor, a novel potent targeted therapy, induces cell apoptosis in renal cell carcinoma. *Tumour Biol J Int Soc Oncodev Biol Med*. 2014;35(8):7659–68. doi:10.1007/s13277-014-2022-x.
- Motzer RJ, Hutson TE, Cella D, Reeves J, Hawkins R, Guo J, et al. Pazopanib versus sunitinib in metastatic renal-cell carcinoma. *N Engl J Med*. 2013;369(8):722–31. doi:10.1056/NEJMoa1303989.
- Aebersold R, Mann M. Mass spectrometry-based proteomics. *Nature*. 2003;422(6928):198–207. doi:10.1038/nature01511.
- White NM, Masui O, Desouza LV, Krakovska O, Metias S, Romaschin AD, et al. Quantitative proteomic analysis reveals potential diagnostic markers and pathways involved in pathogenesis of renal cell carcinoma. *Oncotarget*. 2014;5(2):506–18.
- Sangawa A, Shintani M, Yamao N, Kamoshida S. Phosphorylation status of Akt and caspase-9 in gastric and colorectal carcinomas. *Int J Clin Exp Pathol*. 2014;7(6):3312–7.
- Wu YM, Liu CH, Huang MJ, Lai HS, Lee PH, Hu RH, et al. CIGALT1 enhances proliferation of hepatocellular carcinoma cells via modulating MET glycosylation and dimerization. *Cancer Res*. 2013;73(17):5580–90. doi:10.1158/0008-5472.CAN-13-0869.
- Noh SJ, Kang MJ, Kim KM, Bae JS, Park HS, Moon WS, et al. Acetylation status of P53 and the expression of DBC1, SIRT1, and androgen receptor are associated with survival in clear cell renal cell carcinoma patients. *Pathology*. 2013;45(6):574–80. doi:10.1097/PAT.0b013e3283652c7a.
- Chen Y, Zhang J, Lin Y, Lei Q, Guan KL, Zhao S, et al. Tumour suppressor SIRT3 deacetylates and activates manganese superoxide dismutase to scavenge ROS. *EMBO Rep*. 2011;12(6):534–41. doi:10.1038/embor.2011.65.
- Wang Q, Zhang Y, Yang C, Xiong H, Lin Y, Yao J, et al. Acetylation of metabolic enzymes coordinates carbon source utilization and metabolic flux. *Science*. 2010;327(5968):1004–7. doi:10.1126/science.1179687.
- Zhao S, Xu W, Jiang W, Yu W, Lin Y, Zhang T, et al. Regulation of cellular metabolism by protein lysine acetylation. *Science*. 2010;327(5968):1000–4. doi:10.1126/science.1179689.
- Yi C, Ma M, Ran L, Zheng J, Tong J, Zhu J, et al. Function and molecular mechanism of acetylation in autophagy regulation. *Science*. 2012;336(6080):474–7. doi:10.1126/science.1216990.
- Nagaprashantha LD, Talamantes T, Singhal J, Guo J, Vatsyayan R, Rauniyar N, et al. Proteomic analysis of signaling network regulation in renal cell carcinomas with differential hypoxia-inducible factor-2alpha expression. *PLoS One*. 2013;8(8):e71654. doi:10.1371/journal.pone.0071654.
- Ramakrishnan S, Ellis L, Pili R. Histone modifications: implications in renal cell carcinoma. *Epigenomics*. 2013;5(4):453–62. doi:10.2217/epi.13.40.
- Perroud B, Lee J, Valkova N, Dhirapong A, Lin PY, Fiehn O, et al. Pathway analysis of kidney cancer using proteomics and metabolic profiling. *Mol Cancer*. 2006;5:64. doi:10.1186/1476-4598-5-64.
- Parviainen VI, Joenvaara S, Tohmola N, Renkonen R. Label-free mass spectrometry proteome quantification of human embryonic kidney cells following 24 h of sialic acid overproduction. *Proteome Sci*. 2013;11(1):38. doi:10.1186/1477-5956-11-38.
- Edge SB, Compton CC. The American Joint Committee on Cancer: the 7th edition of the AJCC cancer staging manual and the future of TNM. *Ann Surg Oncol*. 2010;17(6):1471–4. doi:10.1245/s10434-010-0985-4.
- Wu F, Zhao ZH, Ding ST, Wu HH, Lu JJ. High mobility group box 1 protein is methylated and transported to cytoplasm in clear cell renal cell carcinoma. *Asian J Cancer Prev APJCP*. 2013;14(10):5789–95.
- Theron L, Gueugneau M, Coudy C, Viala D, Bijlsma A, Butler-Browne G, et al. Label-free quantitative protein profiling of vastus lateralis muscle during human aging. *Mol Cell Proteomics MCP*. 2014;13(1):283–94. doi:10.1074/mcp.M113.032698.
- Szklarczyk D, Franceschini A, Kuhn M, Simonovic M, Roth A, Minguez P, et al. The STRING database in 2011: functional interaction networks of proteins, globally integrated and scored. *Nucleic Acids Res*. 2011;39(Database issue):D561–8. doi:10.1093/nar/gkq973.
- Saraon P, Cretu D, Musrap N, Karagiannis GS, Batruch I, Drabovich AP, et al. Quantitative proteomics reveals that enzymes of the ketogenic pathway are associated with prostate cancer progression. *Molecular & cellular proteomics : MCP*. 2013;12(6):1589–601. doi:10.1074/mcp.M112.023887.
- Chu SH, Liu YW, Zhang L, Liu B, Li L, Shi JZ, et al. Regulation of survival and chemoresistance by HSP90AA1 in ovarian cancer SKOV3 cells. *Mol Biol Rep*. 2013;40(1):1–6. doi:10.1007/s11033-012-1930-3.
- Lebdai S, Verhoest G, Parikh H, Jacquet SF, Bensalah K, Chautard D, et al. Identification and validation of TGFBI as a promising prognosis marker of clear cell renal cell carcinoma. *Urol Oncol*. 2014. doi:10.1016/j.urolonc.2014.06.005.
- Amer E, Forrest AR, Ehrlund A, Mejhert N, Itoh M, Kawaji H, et al. Ceruloplasmin is a novel adipokine which is overexpressed in adipose tissue of obese subjects and in obesity-associated cancer cells. *PLoS One*. 2014;9(3):e80274. doi:10.1371/journal.pone.0080274.
- Saraon P, Trudel D, Kron K, Dmitromanolakis A, Trachtenberg J, Bapat B, et al. Evaluation and prognostic significance of ACAT1 as a marker of prostate cancer progression. *Prostate*. 2014;74(4):372–80. doi:10.1002/pros.22758.
- Dhar SK, St Clair DK. Manganese superoxide dismutase regulation and cancer. *Free Radic Biol Med*. 2012;52(11–12):2209–22. doi:10.1016/j.freeradbiomed.2012.03.009.
- Kim HS, Patel K, Muldoon-Jacobs K, Bisht KS, Aykin-Burns N, Pennington JD, et al. SIRT3 is a mitochondria-localized tumor suppressor required for maintenance of mitochondrial integrity and metabolism during stress. *Cancer Cell*. 2010;17(1):41–52. doi:10.1016/j.ccr.2009.11.023.
- Haapalainen AM, Merilainen G, Pirila PL, Kondo N, Fukao T, Wierenga RK. Crystallographic and kinetic studies of human mitochondrial acetoacetyl-CoA thiolase: the importance of potassium and

- chloride ions for its structure and function. *Biochemistry*. 2007;46(14):4305–21. doi:10.1021/bi6026192.
34. Fan J, Shan C, Kang HB, Elf S, Xie J, Tucker M, et al. Tyr phosphorylation of PDP1 toggles recruitment between ACAT1 and SIRT3 to regulate the pyruvate dehydrogenase complex. *Mol Cell*. 2014;53(4):534–48. doi:10.1016/j.molcel.2013.12.026.
 35. Weydert CJ, Waugh TA, Ritchie JM, Iyer KS, Smith JL, Li L, et al. Overexpression of manganese or copper-zinc superoxide dismutase inhibits breast cancer growth. *Free Radic Biol Med*. 2006;41(2):226–37. doi:10.1016/j.freeradbiomed.2006.03.015.
 36. Dhar SK, Tangpong J, Chaiswing L, Oberley TD, St Clair DK. Manganese superoxide dismutase is a p53-regulated gene that switches cancers between early and advanced stages. *Cancer Res*. 2011;71(21):6684–95. doi:10.1158/0008-5472.CAN-11-1233.
 37. Quiros I, Sainz RM, Hevia D, Garcia-Suarez O, Astudillo A, Rivas M, et al. Upregulation of manganese superoxide dismutase (SOD2) is a common pathway for neuroendocrine differentiation in prostate cancer cells. *International Journal of Cancer Journal International du Cancer*. 2009;125(7):1497–504. doi:10.1002/ijc.24501.
 38. Perry JJ, Hearn AS, Cabelli DE, Nick HS, Tainer JA, Silverman DN. Contribution of human manganese superoxide dismutase tyrosine 34 to structure and catalysis. *Biochemistry*. 2009;48(15):3417–24. doi:10.1021/bi8023288.
 39. Qiu X, Brown K, Hirschey MD, Verdin E, Chen D. Calorie restriction reduces oxidative stress by SIRT3-mediated SOD2 activation. *Cell Metab*. 2010;12(6):662–7. doi:10.1016/j.cmet.2010.11.015.
 40. Huang P, Feng L, Oldham EA, Keating MJ, Plunkett W. Superoxide dismutase as a target for the selective killing of cancer cells. *Nature*. 2000;407(6802):390–5. doi:10.1038/35030140.
 41. Carew JS, Huang P. Mitochondrial defects in cancer. *Mol Cancer*. 2002;1:9.
 42. Mitrakas AG, Kalamida D, Koukourakis MI. Effect of mitochondrial metabolism-interfering agents on cancer cell mitochondrial function and radio/chemosensitivity. *Anti-Cancer Drugs*. 2014. doi:10.1097/CAD.0000000000000152.
 43. Wang Y, Zhang R, Wu D, Lu Z, Sun W, Cai Y, et al. Epigenetic change in kidney tumor: downregulation of histone acetyltransferase MYST1 in human renal cell carcinoma. *Journal of experimental & clinical cancer research : CR*. 2013;32:8. doi:10.1186/1756-9966-32-8.
 44. Juengel E, Dauselt A, Makarevic J, Wiesner C, Tsaor I, Bartsch G, et al. Acetylation of histone H3 prevents resistance development caused by chronic mTOR inhibition in renal cell carcinoma cells. *Cancer Lett*. 2012;324(1):83–90. doi:10.1016/j.canlet.2012.05.003.
 45. Kanao K, Mikami S, Mizuno R, Shinojima T, Murai M, Oya M. Decreased acetylation of histone H3 in renal cell carcinoma: a potential target of histone deacetylase inhibitors. *J Urol*. 2008;180(3):1131–6. doi:10.1016/j.juro.2008.04.136.